Evaluation of 4-Borono-2-^{18}F-Fluoro-L-Phenylalanine-Fructose as a Probe for Boron Neutron Capture Therapy in a Glioma-Bearing Rat Model

Hsin-Ell Wang, PhD[1]; Ai-Ho Liao, MS[1]; Win-Ping Deng, PhD[2]; Pi-Fang Chang, MS[1]; Jyh-Cheng Chen, PhD[1]; Fu-Du Chen, PhD[1]; Ren-Shen Liu, MD[3]; Jin-Shin Lee, PhD[1]; and Jeng-Jong Hwang, PhD[1]

[1]Department of Medical Radiation Technology and Institute of Radiological Sciences, National Yang-Ming University, Taipei, Taiwan; [2]Institute of Biomedical Science, Taipei Medical University, Taipei, Taiwan; and [3]National PET and Cyclotron Center, Veterans General Hospital, Taipei, Taiwan

L-*p*-Boronophenylalanine (BPA) has been applied as a potential boron carrier for the treatment of malignant glioma in clinical boron neutron capture therapy (BNCT) since 1994. To provide the pharmacokinetics of BPA for clinical use of BNCT in Taiwan, 4-borono-2-^{18}F-fluoro-L-phenylalanine-fructose (^{18}F-FBPA-Fr) was synthesized and the biologic characteristics of this radiotracer in glioma-bearing rats were investigated. **Methods:** Radiolabeled ^{18}F-F_2 was produced via the $^{20}Ne(d,\alpha)^{18}F$ reaction, and ^{18}F-acetyl hypofluorite (^{18}F-AcOF) was generated by passing ^{18}F-F_2 through a column filled with tightly packed KOAc/HOAc powder. The effluent containing ^{18}F-AcOF was bubbled into BPA in trifluoroacetic acid, then purified by high-performance liquid chromatography, and further composited with fructose to afford ^{18}F-FBPA-Fr. Male Fischer 344 rats bearing F98 glioma in the left brain were used for biologic studies. The biodistribution of BPA-Fr and ^{18}F-FBPA-Fr was determined, and the microautoradiography and PET imaging of ^{18}F-FBPA-Fr were performed, on the 13th day after tumor inoculation. **Results:** The radiochemical purity of ^{18}F-FBPA-Fr was >97% and the radiochemical yield of ^{18}F-FBPA-Fr was 20%–25%. In glioma-bearing rats, the accumulation ratios of B-10 for glioma-to-normal brain were 2.05, 1.86, 1.24, and 1.10 at 0.5, 1, 2, and 4 h, respectively, after administration of 43 mg BPA-Fr via the tail vein. The accumulation ratios of ^{18}F-FBPA-Fr for glioma-to-normal brain were 3.45, 3.13, 2.61, and 2.02, whereas the tumor-to-heart blood ratios were 1.72, 2.61, 2.00, and 1.93, respectively, for the same time points. The uptake characteristics of BPA-Fr and ^{18}F-FBPA-Fr in F98 glioma were similar with a maximum at 1 h after the drugs' administration. The results obtained from the biodistribution studies indicated that 0.5–1 h after BPA-Fr injection would be the optimal time for BNCT. Biodistribution, PET images, and brain microautoradiography of ^{18}F-FBPA-Fr all confirmed this finding. **Conclusion:** ^{18}F-FBPA-Fr showed specific tumor uptake in F98 glioma-bearing rats and could be used as a probe for BPA-Fr in BNCT. This study provides useful information for the future clinical application of BNCT in brain tumor therapy.

Key Words: boron neutron capture therapy; 4-borono-2-^{18}F-fluoro-L-phenylalanine-fructose; F98 glioma; microautoradiography; PET

J Nucl Med 2004; 45:302–308

The basic concept of a binary system for cancer treatment is to selectively destroy malignant cells while concomitantly sparing normal tissues (*1*,*2*). Boron neutron capture therapy (BNCT) is one of the binary cancer treatment systems that is based on the selective accumulation of ^{10}B in tumors and then irradiation with a neutron source. The selective accumulation of ^{10}B in tumors and the subsequent capture of an epithermal neutron by a ^{10}B atom eject an α-particle (He^{2+}) and a lithium nucleus (^{7}Li) in opposite directions. The average track of these densely ionizing particles is approximately 14 μm, about the diameter of one cell, so that killing of tumor cells is highly efficient (*3*). BNCT has been proposed for the treatment of human gliomas since 1936 (*4*). Clinical trials are presently conducted in the United States, Japan, and Europe using reactor-generated epithermal neutron beams and ^{10}B-containing compounds such as sulfhydryl borane ($Na_2B_{12}H_{11}SH$) and L-*p*-boronophenylalanine (BPA) (*5*–*7*).

In Taiwan, the reactor at National Tsing-Hua University (THOR) is under remodeling and will be upgraded as a dedicated facility for BNCT with an ultimate goal to perform clinical trials for the treatment of gliomas and hepatomas. The success of BNCT depends mainly on the differential uptake of the boronated compound in tumors compared with that in surrounding normal tissues to ensure a high ratio (about 3:1) of uptake of boron in tumors (*8*). BPA conjugated with fructose has been proven to increase

Received Apr. 7, 2003; revision accepted Oct. 9, 2003.

For correspondence or reprints contact: Jeng-Jong Hwang, PhD, Department of Medical Radiation Technology, Institute of Radiological Sciences, National Yang-Ming University, 155 Li-Nong St., Section 2, Pei-tou, Taipei 112, Taiwan.

E-mail: jjhwang@ym.edu.tw

its solubility, so that the drug uptake in tumor is enhanced (*9,10*).

In this study, we used 4-borono-2-^{18}F-fluoro-L-phenylalanine-fructose (^{18}F-FBPA-Fr) as a scintillation probe of BPA to study the pharmacokinetics of this drug in F98 glioma-bearing Fischer 344 rats. The ^{10}B content in tumor and normal tissues or organs of glioma-bearing rats at different time points after intravenous administration of both ^{18}F-FBPA-Fr and BPA-Fr was determined by inductively coupled plasma mass spectroscopy (ICP-MS). The biodistribution of ^{18}F-FBPA-Fr was determined with γ-scintillation counting of removed tissues and by microautoradiography. PET scanning of ^{18}F-FBPA-Fr injected rats was also performed.

MATERIALS AND METHODS

Preparation of ^{18}F-FBPA-Fr

^{18}F-FBPA-Fr was prepared using the method as described previously by Imahori et al. with some modifications (*11*). Radiolabeled ^{18}F-F_2 was produced through the ^{20}Ne(d,α)^{18}F reaction using a Scanditronix MC17F cyclotron in the National PET and Cyclotron Center (Veterans General Hospital, Taipei, Taiwan). About 5.55 GBq ^{18}F-F_2 were produced from Ne mixed with 200 μmol of carrier F_2 in an aluminum target body irradiated with 8.5-MeV deuteron for 2 h at 30-μA beam current. ^{18}F-Acetyl hypofluorite (^{18}F-AcOF) was generated by passing ^{18}F-F_2 through a 5.6 × 35 mm (inside diameter [ID]) cartridge containing 500 mg of tightly packed KOAc/HOAc powder (1:1.5) prepared as described by Jewett et al. (*12*). The effluent from the cartridge was bubbled (flow rate, 40 mL/min) into a 5-mL conical Reacti vial containing BPA (20 mg, 100 μmol; New Concept Therapeutics, Inc.) in 4-mL trifluoroacetic acid at ambient temperature. The trifluoroacetic acid was removed under reduced pressure. Acetic acid (0.1%, 2 mL) was used to dissolve the residue and then filtered through a 0.22-μm membrane filter (Millex-GV [reference no. SLGVR25LS]; Millipore Corp.). The ^{18}F-FBPA was purified by a reverse-phase high-performance liquid chromatography (HPLC) separation system. The preparative HPLC system includes a radial compression module (RCM; Waters Corp.) containing a Delta-Pak C_{18} guard cartridge and column (25 × 10 mm ID length and 25 × 100 mm ID, respectively), an ultraviolet detector (Waters 486 tunable absorbance detector; Waters Corp.), and a radioactivity detector (Bioscan, Inc.). Acetic acid (0.1%) was used as the mobile phase (flow rate, 10 mL/min). The ^{18}F-FBPA that eluted between 24 and 29 min was collected, and the radiochemical purity was determined with analytic HPLC (100-RP-18, 5 μm, 4 × 250 mm column [LiChrospher]; eluent, methanol/0.8% acetic acid containing 1 mmol/L ethylenediaminetetraacetic acid and 1 mmol/L octyl sodium sulfate [15:85, v/v]; flow rate, 1 mL/min). The solvent was removed under reduced pressure; then sodium bicarbonate (0.5 mL, 8.4%) and fructose (1.0 mL, 0.5 mol/L) were added and the solution was filtered through a 0.22-μm membrane filter (Millex-GV [reference no. SLGV013SL]; Millipore Corp.) into a sterile vial to afford the final product of ^{18}F-FBPA-Fr. The overall synthetic time was 110 min.

F98 Glioma Brain Tumor Model in Rats

Male Fischer 344 rats (12–14 wk old, about 250–280 g) were anesthetized intraperitoneally with a mixture of ketamine and xylazine. Then 1 × 10^5 F98 rat glioma cells (a generous gift from Dr. Rolf F. Barth, Ohio State University) in 10 μL Hanks' balanced salt solution without Mg^{2+} and Ca^{2+} were injected into the left brain region. F98 cells were slowly (15–20 s) injected into the brain, the syringe was held still for 2 min, and the needle was then withdrawn. The hole was sealed with bone wax. Finally, the wound was flushed with iodinated alcohol and held together with a sterilized steel clip. The animal experiments were approved by the Laboratory Animal Care Panel of National Yang Ming University.

Biodistribution of ^{18}F-FBPA-Fr in F98 Glioma-Bearing Fischer 344 Rats

The biodistribution of ^{18}F-FBPA-Fr was determined on the 13th day after tumor implantation. Tumor-bearing rats weighing 250–280 g, anesthetized with ether (catalog no. 100946B; Merck), were injected with 8.15–10.0 MBq ^{18}F-FBPA-Fr through lateral tail veins. At 0.5, 1, 2, and 4 h after injection, rats were killed with chloroform (catalog no. 1.02445; Merck). Tumors, surrounding normal brain tissues, pancreas, blood, kidneys, small intestine, spleen, and liver were removed, and parts of these tissues or organs were assayed for radioactivity with a γ-scintillation counter (Cobra II Autogamma; Packard). The uptake of ^{18}F-FBPA-Fr in tissues or organs was expressed in counts per minute (cpm) corrected with decay and normalized as the percentage injected dose per gram of tissue (%ID/g) according to the following formula:

$$\%\mathrm{ID/g} = \frac{A_0 \times 1{,}000}{\mathrm{ID}\ (\mu\mathrm{Ci}) \times 3.7 \times 10^4 \times 60 \times \mathrm{Eff} \times \mathrm{organ\ weight\ (mg)}},$$

where $\ln(A/A_0) = -0.693t/t_{1/2}$, A = radioactivity (cpm) of tissues or organs measured by γ-counter, A_0 = decay-corrected radioactivity (cpm) of tissues or organs, Eff = counting efficiency of γ-scintillation counter, $t_{1/2}$ = half-life of radioisotope, and t = time after injection.

^{10}B Assay in F98 Glioma-Bearing Fischer 344 Rats After BPA-Fr or ^{18}F-FBPA-Fr Injection

The ^{10}B assay was performed with the same animal model and administration route of both drugs. Test substances (172 mg/kg body weight for BPA-Fr and 8.15–10.0 MBq for ^{18}F-FBPA-Fr) were injected via the tail vein. The ^{10}B concentrations in tumor and tissues were determined by ICP-MS and were normalized as μg/g of tissue.

Microautoradiography

At 0.5, 1, 2, and 4 h after ^{18}F-FBPA-Fr injection, rats were killed with chloroform, and whole brains were surgically removed, frozen immediately with dry ice, and then embedded with Tissue-Tek OCT (optimal cutting temperature) compound (catalog no. 4583; Sakura Finetechnical Co., Ltd.) on round specimen disks (diameter, 2.2 cm). The embedded samples were placed on a −30°C freezing stage in the cryostat (CM 3050; Leica) for about 30 min. The coronal sectioning was performed with a slice thickness of 15 μm. Sections attached on the microscopic slides were air dried at room temperature and applied to imaging plates (BAS cassette 2040; Fujifilm) and exposed for about 36 h. After exposure, the imaging plates were assayed with a BAS-2500 IP reader (Fuji Photo Film Co.).

Quantification of ^{18}F-FBPA-Fr Biodistribution in Microautoradiography

After scanning the microautoradiographic sections, the images were measured by a bioimage reader connected to a Pentium IV

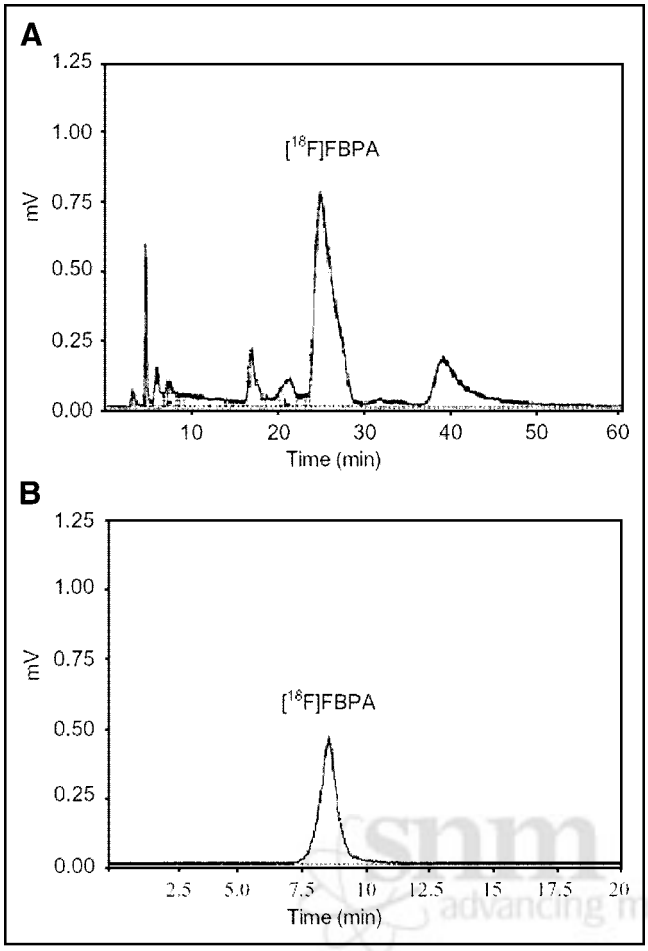

FIGURE 1. HPLC chromatograms of ^{18}F-FBPA solution. (A) Crude product, determined with preparative HPLC: retention time of ^{18}F-FBPA was about 24.9 min. (B) Purified product, determined with analytic HPLC: retention time of ^{18}F-FBPA was about 8.6 min.

computer where images were stored in TIF format. The specificities of the reading conditions were as follows: resolution of 50, gradation of 16 bits, dynamic range of L5, and sensitivity of 10,000. The stored images were analyzed with Adobe Photoshop 6.0. The regions of interest (ROIs) were fixed at 1,643 pixels to obtain the average optical density (OD) for each ROI measured. Repeated measurements for ANOVA were applied to find the statistical significance of the results.

PET Scanning

PET images of F98 glioma-bearing rats were obtained using an ECAT HR+ PET system (Siemens/CTI) that produced 63 image slices over a 15.52-cm axial field of view. The spatial resolution is 4.6 mm in the central axis using the 2-dimensional brain mode. PET scanning was performed on the 13th day after tumor implantation. Each tumor-bearing rat was anesthetized with halothane vapor using a vaporizer system (Fluosorber; Int. Market Supply) and injected with 20.35-MBq ^{18}F-FBPA-Fr through a lateral tail vein. Data acquisition by PET scanning was initiated at the first minute after drug injection. Dynamic coronal images were acquired using ten 60-s frames and ten 2-min frames, followed by 10-min frames up to 4 h after injection. Transverse scanning was

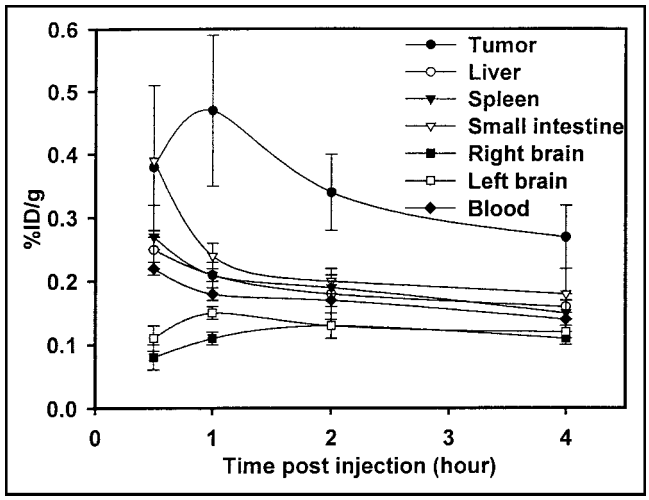

FIGURE 2. Time–activity curves of ^{18}F-FBPA-Fr in various organs of F98 glioma-bearing Fischer 344 rats after intravenous injection (8.15–10.0 MBq).

also performed at 4 h after injection. All images were reconstructed using the weighted attenuation method, ordered-subsets expectation maximization, with 128 × 128 pixel image size, 16 subsets, a zoom factor of 5, and use of a gaussian filter.

Time–activity curves were plotted for both tumor and reference ROIs, located in the contralateral normal brain. ROIs of tumor were drawn from each image plane in which tumor was visible on the final time frame. The radioactivities of tumor ROIs at different time frames were calculated. Reference ROIs were drawn from the final frame at the end of scanning in the contralateral normal brain and applied to all images in the dynamic sequence.

RESULTS

Preparation of ^{18}F-FBPA-Fr

The radiochemical purity of purified ^{18}F-FBPA was >97% as determined with HPLC (Fig. 1). The radio-

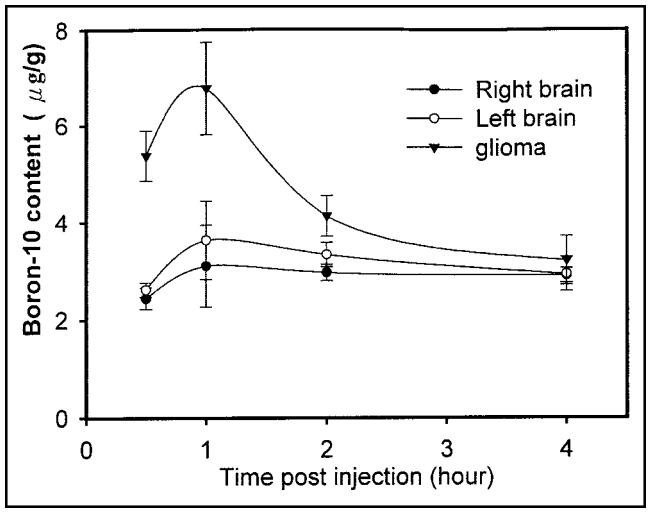

FIGURE 3. ^{10}B concentration in various organs of F98 glioma-bearing Fischer 344 rats assayed by ICP-MS. Injection dose of BPA-Fr was 43 mg per rat.

TABLE 1
Biodistribution of ^{18}F-FBPA-Fr in Tumor, Left Brain, Right Brain, and Blood of F98 Glioma-Bearing Fischer 344 Rats at 0.5, 1, 2, and 4 Hours After Intravenous Injection of 8.15–10.0 MBq ^{18}F-FBPA-Fr

Time (h)	%ID/g ± SD				Ratio	
	T	LT	RT	Blood	T/LT	T/blood
0.5	0.38 ± 0.13	0.11 ± 0.02	0.08 ± 0.02	0.22 ± 0.01	3.45	1.72
1	0.47 ± 0.12	0.15 ± 0.01	0.11 ± 0.01	0.18 ± 0.01	3.13	2.61
2	0.34 ± 0.06	0.13 ± 0.02	0.13 ± 0.02	0.17 ± 0.03	2.61	2.00
4	0.27 ± 0.05	0.12 ± 0.01	0.11 ± 0.01	0.14 ± 0.01	2.25	1.93

T = tumor implanted in L brain region; LT = L brain; RT = R brain.

chemical yield of ^{18}F-FBPA-Fr (444–518 MBq corrected to end of bombardment [EOB] based on the radioactivity of ^{18}F-AcOF) was 20%–25% after about 10 runs.

Biodistribution of ^{18}F-FBPA-Fr in F98 Glioma-Bearing Fischer 344 Rats

The uptake of ^{18}F-FBPA-Fr in F98 glioma reached the maximum level at 1 h after injection (Figs. 2and 3; Table 1). Although the tumor-to-heart blood ratio showed a steady 2-fold uptake during the 4-h study (1.72, 2.61, 2.00, and 1.93 at 0.5, 1, 2, and 4 h after ^{18}F-FBPA-Fr injection), the tumor-to-normal brain ratio reached the maximum earlier (3.45 at 0.5 h after injection) and decreased slowly with time (3.13, 2.61, and 2.25 at 1, 2, and 4 h after injection). The biodistribution of ^{18}F-FBPA-Fr for the other tissues or organs after a single injection of ^{18}F-FBPA-Fr is also shown in Figure 2 and Table 2. The tumor uptake reached the maximum (0.47 ± 0.12 %ID/g) at 1 h after intravenous injection of ^{18}F-FBPA-Fr and dropped to 0.27 ± 0.05 %ID/g at 4 h after injection. The kidneys had the highest radioactivity levels and pancreas had the second highest radioactivity levels up to 4 h after injection.

^{10}B Assay in F98 Glioma-Bearing Fischer 344 Rats After BPA-Fr and ^{18}F-FBPA-Fr Injection

The ^{10}B content in F98 glioma reached the maximum at 1 h after injection of both BPA-Fr and ^{18}F-FBPA-Fr (Fig. 3; Tables 3 and 4). The result is consistent with that of ^{18}F-FBPA-Fr shown in Table 2. However, tumor-to-left brain ratios were highest at 0.5 h after injection in both cases (Tables 3 and 4).

Brain Microautoradiography

The biodistribution of ^{18}F-FBPA-Fr imaged by microautoradiography in rats bearing F98 gliomas is shown in Figure 4. The higher OD regions (Fig. 4, top) are well correlated with the anatomic localization of the tumors (Fig. 4, bottom). The tumor regions could be detected as viewed by phosphor plate imaging at 0.5 h after injection. The quantification of relative uptake of ^{18}F-FBPA-Fr in tumor and normal brain from microautoradiograms is shown in Figure 5. The accumulation of ^{18}F-FBPA-Fr in tumors from 0.5 to 4 h after drug administration was significantly higher than that of surrounding normal brain tissues, in which 1 h was the highest. The results further confirm that the uptake of ^{18}F-FBPA-Fr was higher in tumor than in surrounding normal brain tissue.

PET Scanning of ^{18}F-FBPA-Fr in F98 Glioma-Bearing Fischer 344 Rats

Coronal views of PET images of F98 glioma-bearing Fischer 344 rats are shown in Figure 6. The glioma in the brain can be clearly demonstrated through uptake of ^{18}F-FBPA-Fr on coronal images. Kidneys again showed the highest radioactivity levels. The time–activity curves

TABLE 2
Biodistribution of ^{18}F-FBPA-Fr in Tumor and Other Normal Tissues of F98 Glioma-Bearing Fischer 344 Rats at 0.5, 1, 2, and 4 Hours After Intravenous Injection of 8.15–10.0 MBq ^{18}F-FBPA-Fr

Organ	%ID/g ± SD			
	0.5 h	1 h	2 h	4 h
Tumor	0.38 ± 0.13	0.47 ± 0.12	0.34 ± 0.06	0.27 ± 0.05
Liver	0.25 ± 0.03	0.21 ± 0.01	0.18 ± 0.02	0.16 ± 0.01
Spleen	0.27 ± 0.05	0.21 ± 0.02	0.19 ± 0.02	0.15 ± 0.03
Kidney	2.46 ± 0.27	2.24 ± 0.29	2.14 ± 0.28	1.86 ± 0.13
Pancreas	1.17 ± 0.19	0.88 ± 0.04	0.83 ± 0.08	0.69 ± 0.02
Small intestine	0.39 ± 0.12	0.24 ± 0.02	0.20 ± 0.02	0.18 ± 0.04

TABLE 3
^{10}B Concentration of Tumor, Left Brain, and Right Brain in F98 Glioma-Bearing Fischer 344 Rats at 0.5, 1, 2, and 4 Hours After Intravenous Injection of BPA-Fr (172 mg/kg)

Time (h)	^{10}B concentration (μg/g tissue)			Ratio
	T	LT	RT	T/LT
0.5	5.38 ± 0.52	2.62 ± 0.15	2.44 ± 0.22	2.05
1	6.78 ± 0.96	3.64 ± 0.81	3.11 ± 0.84	1.86
2	4.13 ± 0.42	3.34 ± 0.25	2.97 ± 0.17	1.24
4	3.22 ± 0.50	2.94 ± 0.35	2.91 ± 0.15	1.10

T = tumor implanted in L brain region; LT = L brain; RT = R brain. Three rats were studied at each time point.

TABLE 4
^{10}B Concentration of Tumor, Left Brain, and Right Brain in F98 Glioma-Bearing Fischer 344 Rats at 0.5, 1, 2, and 4 Hours After Intravenous Injection of 8.15–10.0 MBq ^{18}F-FBPA-Fr

Time (h)	^{10}B concentration (nmol/g tissue)			Ratio
	T	LT	RT	T/LT
0.5	2.97 ± 1.02	0.86 ± 0.16	0.62 ± 0.16	3.45
1	3.67 ± 0.94	1.17 ± 0.08	0.86 ± 0.08	3.13
2	2.66 ± 0.47	1.02 ± 0.16	1.02 ± 0.16	2.61
4	2.11 ± 0.39	0.94 ± 0.08	0.86 ± 0.08	2.02

T = tumor implanted in L brain region; LT = L brain; RT = R brain. Six rats were studied at each time point.

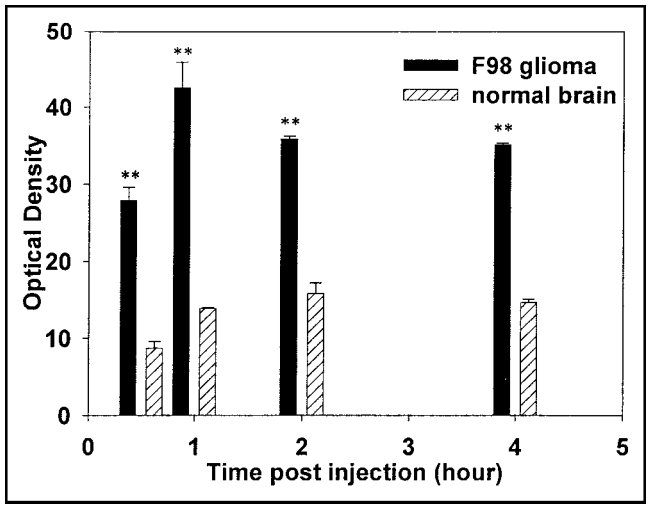

FIGURE 5. Relative optical densities of tumor and surrounding normal brain derived from microautoradiography as shown in Figure 4. $^{**}P < 0.01$.

of ^{18}F-FBPA-Fr in both tumor and normal brain are shown in Figure 7, which demonstrated that the accumulation of radioactivity in tumor was increased rapidly at first hour and then gradually declined up to 4 h after drug injection.

DISCUSSION

The methodology of BNCT is complicated in 2 respects: neutron dosimetry and the neutron-capturing efficiency of boron compounds. Each component could be manipulated independently, so that the optimal time between administration of the neutron capture agent and neutron irradiation can be adjusted for differential uptake of ^{10}B between tumor and normal tissues. Since ^{10}B accumulation varies with the nature of the tumor, which even with the same grades often varies in their biochemical properties, it is suggested that the ^{10}B concentration in tumors should be determined for each individual patient before neutron irradiation. The collection of accurate data for individual patients is very important for performing BNCT and neutron dosimetry. ^{10}B levels in tumor and surrounding normal brains in vivo play a key role in BNCT (*13*). Nonetheless, assay of the time–activity curve of the ^{10}B concentration in tumor and normal tissues often is not easy to perform. A noninvasive method for the boron distribution assay would be valuable to patients who are in poor surgical condition. Imahori et al. designed a method for quantitative measurement of ^{10}B concentration in patients with high-grade gliomas by PET imaging with ^{18}F-FBPA (*13*). According to their study, the estimated values of ^{10}B concentration in gliomas were very close to those of the ^{10}B concentration in surgical specimens based on the incorporation constant (*Ic**). This method was based solely on PET imaging and could potentially provide data that would assist in the selection of patients for the BNCT treatment after surgical resection of brain tumors. Ishiwata et al. also demonstrated that the uptake of ^{10}B-BPA was similar to that of ^{18}F-FBPA in pharmacokinetics. The concentration of L-BPA in tumor and normal tissues assayed by ICP-MS corresponded almost 1:1 in hamsters receiving ^{18}F-FBPA (*14*).

BPA has been reported to be a safe agent in BNCT for glioma patients (*15*). Neither toxicity resulting from the intravenous infusion of 250–290 mg/kg of BPA-Fr nor radiation-induced tissue damage caused by neutrons has been reported. The high uptake of ^{18}F-FBPA-Fr in the pancreas of rat was also found in this study, which is consistent with the finding in mice as previously reported by Ishiwata et al. (*16*). Thus, ^{18}F-FBPA-Fr could be also ap-

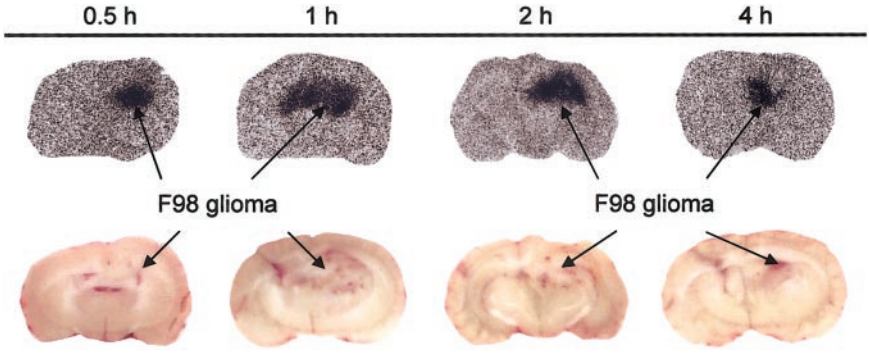

FIGURE 4. Microautoradiography of brains in F98 glioma-bearing Fischer 344 rats after intravenous injection of 54.76-MBq ^{18}F-FBPA-Fr. Times after drug administration are indicated.

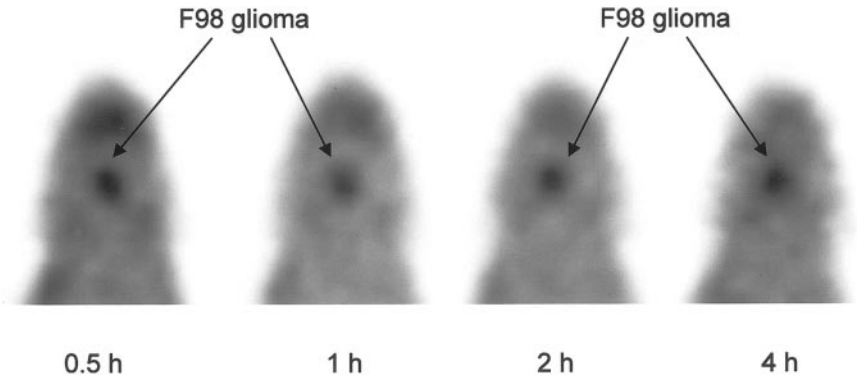

FIGURE 6. PET images of F98 glioma-bearing Fischer 344 rat at 0.5, 1, 2, and 4 h after intravenous injection of 20.35 MBq-^{18}F-FBPA-Fr (coronal view).

plied in evaluating the function of the pancreas by PET imaging. The ^{10}B content in glioma and normal brain after administration of BPA-Fr was parallel to that of ^{18}F-FBPA-Fr, suggesting that the ^{10}B content in various tissues or organs could also be estimated from the uptake of ^{18}F-FBPA-Fr in normal tissues or organs after administration of ^{18}F-FBPA-Fr. This may be an advantage of PET scanning as a tool in monitoring the drug distribution for optimal neutron irradiation time in BNCT.

Microautoradiography of tumors showed that the high OD regions were well correlated with the localization of gliomas. This technique also demonstrated that tumor had higher uptakes of ^{18}F-FBPA-Fr than that of normal brain. Gliomas could also be visualized in dynamic PET imaging. The kidneys and pancreas both showed high radioactivity levels. The time–activity curves of tumor and normal brain tissues derived from dynamic PET images also showed that the radioactivity of the tumor reached the maximum at 1 h after drug injection and then decreased with the increase in time. The results were also consistent with the findings from the biodistribution study. The noninvasive PET assay of the concentration of the positron-emitted radioisotope-labeled compounds—such as ^{18}F-FBPA-Fr in tumors and normal tissues in vivo—not only provides images of tumors but also allows determination of the concentration of the atom of interest in various tissues or organs if the calibration curve of the biodistribution study is investigated in parallel, such as the pharmacologic characteristics of ^{18}F-FBPA-Fr and BPA-Fr.

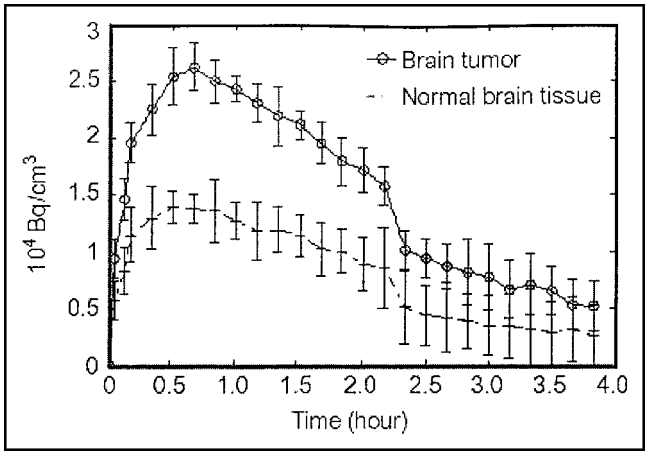

FIGURE 7. Time–activity curve of tumor and normal brain tissue in F98 glioma-bearing Fischer 344 rat derived from PET images after intravenous injection of 20.35-MBq ^{18}F-FBPA-Fr.

CONCLUSION

^{18}F-FBPA-Fr shows high tumor-to-normal tissue uptake ratio in F98 glioma-bearing rats and can be used as a probe for BPA-Fr in BNCT for the treatment of brain tumors. This study provides useful information for the future clinical application of BNCT in cancer therapy.

ACKNOWLEDGMENTS

This study was supported by grants NSC89-2745-P-010-003, NSC91-2745-P-010-003 and NSC92-2745-P-010-002 from National Science Council, Taipei, Taiwan. We thank the staff of the National PET and Cyclotron Center in Taipei Veterans General Hospital, who kindly provided the radiopharmaceuticals. The PET Gene Probe Core of National PET/Cyclotron Center, Veterans General Hospital, Taipei, Taiwan, is also gratefully acknowledged. We also thank the staff of the Instrumentation Center at the National Tsing Hua University, Hsinchu, Taiwan, for technical support of the tissue boron concentration assay. The imaging instrument (FLA5000, Fuji Photo Film Co.) was supported by grant 89-B-FA22-1-4-05 to the National Yang-Ming University, Taipei, Taiwan, for promoting academic excellence of universities from the Ministry of Education of Taiwan. Part of this study was presented at the 10th International Congress on Neutron Capture Therapy in Essen, Germany, September 8–13, 2002.

REFERENCES

1. Slatkin DN. A history of boron neutron capture therapy of brain tumors: postulation of a brain radiation dose tolerance limit. *Brain*. 1991;114:1609–1629.
2. Barth RF, Soloway AH, Fairchild RO, Brugger RM. Boron neutron capture therapy for cancer: realities and prospects. *Cancer*. 1992;70:2995–3007.
3. Coderre JA, Chanana AD, Joel DD, et al. Biodistribution of boronophenylalanine in patients with glioblastoma multiforme: boron concentration correlates with tumor cellularity. *Radiat Res*. 1998;149:163–170.

4. Locher GL. Biological effects and therapeutic possibilities of neutrons. *AJR.* 1936;36:1–13.
5. Hatanaka H, Nakagawa Y. Clinical results of long surviving brain tumor patients who underwent boron neutron capture therapy. *Int J Radiat Oncol Biol Phys.* 1994;28:1061–1066.
6. Diaz AZ. Assessment of the results from the phase I/II boron neutron capture therapy trials at the Brookhaven National Laboratory from a clinician's point of view. *J Neurooncol.* 2003;62:101–109.
7. Hideghety K, Sauerwein W, Haselsberger K, et al. Postoperative treatment of glioblastoma with BNCT at the Petten irradiation facility. *Strahlenther Onkol.* 1999;175(suppl 2):111–114.
8. Soloway AH, Tjarks W, Barnum BA, et al. The chemistry of neutron capture therapy. *Chem Rev.* 1998;98:1515–1562.
9. Yoshino K, Suzuki A, Mori Y, et al. Improvement of solubility of p-boronophenylalanine by complex formation with monosaccharides. *Strahlenther Onkol.* 1989;165:127–129.
10. Honda C, Shiono M, Wadabayashi N, et al. Increased selective ^{10}B-uptake in malignant melanoma using systemic administration of ^{10}B-BPA-fructose complex. In: Allen BJ, Moore DE, Harrington BV, eds. *Progress in Neutron Capture Therapy for Cancer.* New York, NY: Plenum Press; 1992:421–424.
11. Imahori Y, Ueda S, Ohmori Y, et al. Fluorine-18-labeled fluoroboronophenylalanine PET in patients with glioma. *J Nucl Med.* 1998;39:325–333.
12. Jewett DM, Potocki JF, Ehrenkaufer RE. A gas-solid phase microchemical method for the synthesis of acetyl hypofluorite. *J Fluor Chem.* 1984;38:477–484.
13. Imahori Y, Ueda S, Ohmori Y, et al. Positron emission tomography-based boron neutron capture therapy using boronophenylalanine for high-grade gliomas: Part I. *Clin Cancer Res.* 1998;4:1825–1832.
14. Ishiwata K, Shinono M, Kubota K, et al. A unique *in vivo* assessment of 4-[^{10}B]borono-L-phenylalanine in tumor tissues for boron neutron capture therapy of malignant melanomas using positron emission tomography and 4-borono-2-[^{18}F]fluoro-L-phenylalanine. *Melanoma Res.* 1992;2:171–179.
15. Coderre JA, Elowitz E, Chadha M, Bergland R, Capala J, Joel DD. Boron neutron capture therapy of glioblastoma multiforme using p-boronophenylalanine and epithermal neutrons: trial design and early clinical results. *J Neurooncol.* 1997; 33:141–152.
16. Ishiwata K, Ido T, Mejia AA, Ichihashi M, Mishima Y. Synthesis and radiation dosimetry of 4-borono-2-[^{18}F]fluoro-D,L-phenylalanine: a target compound for PET and boron neutron capture therapy. *Appl Radiat Isot.* 1991;42:325–328.

snm
advancing molecular imaging